A linear analysis of a two-phase flow model of melt percolation

Stav Gold April 25, 2014

Melt segregation, which is observed in lab experiments and in natural samples, is the phenomenon wherein partially molten rock in the upper mantle spontaneously organizes into melt-rich bands, or lenses, when exposed to shear strain [*Kohlstedt and Holtzman*, 2009]. The phenomenon appears to reduce the viscosity of the aggregate, and may do so in an anisotropic manner. A comprehensive understanding of the effect this has on rock rheology would be useful, especially in improving continuum models of the Earth's viscous deformation. We numerically analyzed plane wave solutions of the linearized versions of the equations governing two-phase flow with the aim of capturing maximal accuracy at the lowest possible computational cost. We then attempted to extend the methods used in this linear analysis to the case of a uniformly random initial condition (RIC), and found that the same methods in this case produced numerical instabilities. In ongoing work, we simulate spontaneous strain-rate driven melt segregation using the full nonlinear equations of motion.

1 Introduction

It has been well known for decades that many geological and seismological phenomena can be explained by the existence of lithospheric plates: relatively rigid, nondeforming regions of Earth's outer layers that move independently. The relative velocities of the plates are of the order of a few tens of millimeters per year. Moreover, a large fraction of all earthquakes and volcanic eruptions occur at plate boundaries, which are seen to be very narrow. However, the physical mechanism responsible for the existence of plates is still not known. While it used to be believed that oceanic lithosphere is brittle to enough to break under convective stress, it has been found that the lithosphere cannot undergo brittle failure at depths exceeding 20km. However, the tectonic plates are generally greater than 100km thick, and so distributed failure mechanisms must be invoked to explain the existence of lithospheric plates.

Continuum models have been successful at generating plates [*Bercovici et al.*, 1969], [*Tackley*, 1998], where the top cold thermal boundary layer produced during thermal convection is not broken, but instead weakens into narrow zones with lateral variations in viscosity. A boundary layer with broad, strong, slowly deforming regions (representing strong plate interiors) separated by narrow zones of weak, rapidly deforming material (representing plate boundaries) is said to have high "plateness," and is considered also to be physically realistic. Simulations including rheological laws that involve self-amplifying viscosity contrasts have shown great success in producing high plateness, implying that physical processes that result in positive feedback of local weakness – referred to as strain-rate weakening (SRW) rheologies – may have had a hand in producing the tectonic plates.

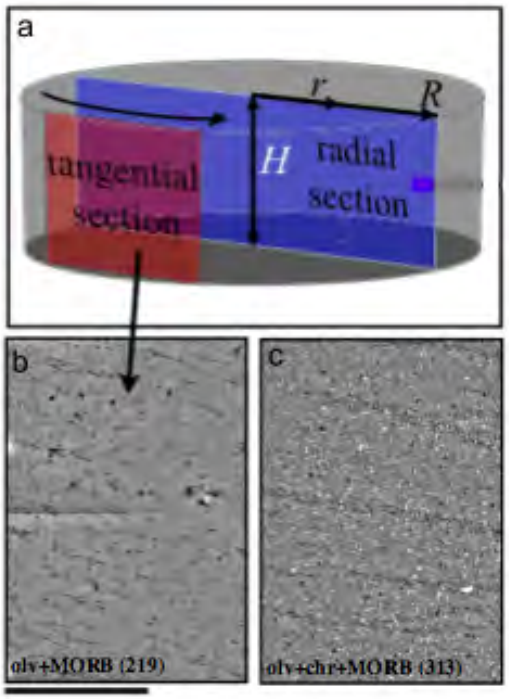

Figure 1: Example of melt banding in experiment. a) Sketch of the torsion sample, illustrating locations of radial and tangential sections. b) Tangential section of an olivine + mid-oceanic ridge basalt (MORB) sample with melt segregation at wavelengths of several grains. c) Tangential section of an olivine + chromite + MORB sample with wider melt bands at longer wavelengths with higher melt fractions [*Holtzman et al.*, 2012]

.

One such promising feedback mechanism is the process of melt band segregation. Rock in the upper mantle may contain a small fraction ($\leq$5% by volume) of a fluid/melt phase. The amount of fluid present in the mantle by volume is equal to the rock's porosity, or melt fraction, ϕ. (Pores are always full of fluid, if they exist; there are no voids

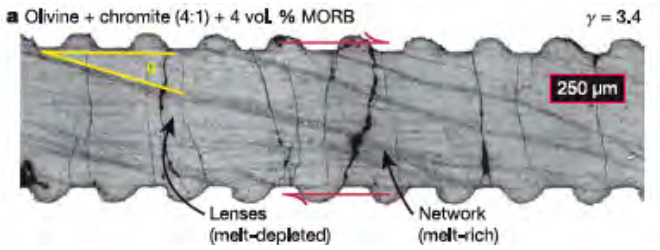

Figure 2: Another example of melt banding in experiment, with 4% volume of liquid-phase MORB [*Katz et al.*, 2006]

.

present in the rock at the pressures of the upper mantle.) This fluid phase has very different material properties from the rock in which it resides; the densities of the respective phases can differ by $\Delta\rho \approx 300\frac{kg}{m^3}$ [*Kohlstedt and Holtzman*, 2009]. It has been shown [*Stevenson*, 1989] that the molten rock that penetrates the porous solid matrix of the upper mantle, starting from a uniformly random distribution, spontaneously generates regular bands of high-porosity regions when the partially molten aggregate is sheared. This is because the melt flows into lower-pressure regions, which are where melt has already accumulated. Major effects on the local viscosity characteristics of the rock ensue, both due to the significant viscosity contrast of the rock's respective phases and the anisotropy created by the melt's spatial organization. We postulate that the effect therefore may have been instrumental in the formation of tectonic plates, and are interested in quantifying the effect's rheological consequences as a means toward preparing a full-scale continuum model simulation employing it.

The following constitutes an analysis of melt segregation's basic features. Following [*Spiegelman*, 2003], we use linearized equations that govern the process and studied the behavior of some simple linear solutions to the full equations.

2 Model and linear perturbation

The equations that govern the motion of the melt phase of rock with respect to its solid phase, ignoring the effect of gravity, are [*Spiegelman*, 2003]:

$$\frac{\delta\phi}{\delta t} + \boldsymbol{\nabla}\cdot[\phi\mathbf{v}] = 0 \tag{1}$$

$$\frac{\delta}{\delta t}(1-\phi) + \boldsymbol{\nabla}\cdot[(1-\phi)\mathbf{V}] = 0 \tag{2}$$

$$\phi(\mathbf{v}-\mathbf{V}) = -\frac{k_\phi}{\mu}[\boldsymbol{\nabla}P - \rho_f\mathbf{g}] \tag{3}$$

$$\boldsymbol{\nabla}P = \boldsymbol{\nabla}\cdot\eta[(\boldsymbol{\nabla}\mathbf{V}) + (\boldsymbol{\nabla}\mathbf{V})^T] + \boldsymbol{\nabla}(\zeta - \frac{2\eta}{3})\boldsymbol{\nabla}\cdot\mathbf{V}) + \bar{\rho}\mathbf{g} \tag{4}$$

Where $\mathbf{v}$ and $\mathbf{V}$ are respectively the melt and solid velocity fields; ϕ is the porosity or melt fraction field; P is the fluid pressure field; $\bar{\rho} = \phi\rho_f + (1-\phi)\rho_s$ is the mean density (where $\rho_f \approx 2700\frac{kg}{m^3}$ and $\rho_s \approx 3000\frac{kg}{m^3}$); k_ϕ is the permeability, which is taken to be a nonlinear function of the porosity; and μ, η and ζ are the fluid viscosity ($\approx$1 Pa s) and the solid's viscosities ($\approx 1\times10^{19-23}$ Pa s).

These equations treat the solid and melt phases as two interpenetrating fluids that have a large viscosity contrast and which are both incompressible. Equations 1 and 2 respectively govern the conservation of melt and solid mass. Equation 3 is the statement of D'Arcy flow, a phenomenologically derived constitutive relation governing the flow of fluid through a porous medium, and Equation 4 is the conservation of momentum.

These equations can be rewritten into the following form, which is more suitable for computation:

$$\frac{\delta\phi}{\delta t} + \mathbf{V}\cdot\boldsymbol{\nabla}\phi = (1-\phi)\mathcal{C} \tag{5}$$

$$\mathcal{C} = \boldsymbol{\nabla}\cdot\frac{k_\phi}{\mu}[\boldsymbol{\nabla}\cdot\eta[(\boldsymbol{\nabla}\mathbf{V}) + (\boldsymbol{\nabla}\mathbf{V})^T] + \boldsymbol{\nabla}(\zeta - \frac{2\eta}{3})\mathcal{C}) \tag{6}$$

$$0 = \boldsymbol{\nabla}\times\boldsymbol{\nabla}\cdot\eta[(\boldsymbol{\nabla}\mathbf{V}) + (\boldsymbol{\nabla}\mathbf{V})^T] \tag{7}$$

where $\mathcal{C} = \boldsymbol{\nabla}\cdot V$ is the compaction rate of the solid velocity field.

Equation 5 is an expansion of equation 2 and shows how the quantity of melt at a point can change: either it is advected there, or, in the case where $\mathcal{C} \neq 0$, the underlying solid matrix is deformed. Equation 6 is a combination of equations 1 through 4 which shows that the solid matrix changes volume as a result of divergence of the melt flux, which occurs only as a result of viscous deformation in the absence of gravitational force. Finally, equation 7 is merely the curl of equation 4, and it

constrains the incompressible component of the flow field.

We consider in this paper only the behavior of the linearized equations–by replacing each field parameter with a constant plus an infinitesimal perturbation, e.g. $\phi = \phi_0 + \epsilon\phi_1, \epsilon \ll 1$. After making this substitution for all parameters, expressing the velocity field perturbation in terms of a compressible and an incompressible component $\mathbf{V}_1 = \boldsymbol{\nabla} \times \vec{\psi}_1^s + \boldsymbol{\nabla} U_1$, and collecting terms of order ϵ, we find the following set of equations for the perturbations after appropriately nondimensionalizing [*Spiegelman*, 2003]:

$$\frac{\delta\phi_1}{\delta t} + y\frac{\delta\phi_1}{\delta x} = (1-\phi_0)\mathcal{C}_1 \tag{8}$$

$$-\nabla^2\mathcal{C}_1 = 2\alpha\xi\frac{\delta^2\phi_1}{\delta x\delta y} \tag{9}$$

$$\nabla^2\mathcal{U}_1 = \mathcal{C}_1 \tag{10}$$

$$\nabla^4\vec{\psi}_1^s = \alpha(\frac{\delta^2\phi_1}{\delta x^2} - \frac{\delta^2\phi_1}{\delta y^2}) \tag{11}$$

where α is the first-order dependence of the viscosity on the porosity. Negative values of α therefore correspond to porosity weakening materials, the class of materials presently under study, and large magnitudes of α correspond to materials which have a viscosity that is strongly dependent on porosity. Although the precise functional form of the dependence of matrix viscosity on porosity is not known–multiple constitutive relations have been proposed, but none have been confirmed–this phrasing of the equations is independent of the functional form of the viscosity $\eta(\phi)$.

We consider a setup of 2D simple shear–a box of aspect ratio 4:1 is sheared along its top and bottom. Periodic boundary conditions are enforced along the left and right edges of the box, and in order to keep the melt inside of the box, Neumann conditions of $\frac{\delta\phi}{\delta y} = 0$ are enforced along the top and bottom boundaries. We impose constant shear strain across the box, and we can therefore use the total strain as a dimensional unit of time, i.e. $t' = \cdot\gamma t$.

3 Linear Perturbation I: Plane Waves

The evolution of these equations is highly dependent upon the initial conditions of the system. As in [*Spiegelman*, 2003], we began by considering the evolution of plane waves. At t=0, we assume that the porosity is given by a plane-wave with a specified orientation $\mathbf{k_0}$ (See figure 3a). Our justification for doing so was that the existence of analytical solutions of the plane-wave amplitude and wave-vector allowed us to use this case as a benchmark for our numerical solution.

Spiegelman's linear analysis predicts that the amplitude of plane-waves evolves as $A(t) = [\frac{1+k^2(0)}{1+k^2(t)}]^{-\alpha\xi(1-\phi_0)}$, where $k^2(t)$ is the magnitude of the wave's wave-vector as a function of time. In the case of simple shear, $\mathbf{k}(t) = k_x^0\mathbf{i} + (k_y^0 - k_x^0 t)\mathbf{j}$, where k_i^0 denotes the initial value of the ith component of the wave-vector. This means that, for $\alpha = 0$, the plane-wave amplitude shouldn't evolve at all, but for $\alpha \neq 0$ the amplitude should grow while the waves make less than a 90° angle with the horizontal and shrink while the waves make more than a 90° angle with the horizontal. Figure 4 gives a comprehensive look at the behavior of the wave amplitudes as a function of time and initial band angle.

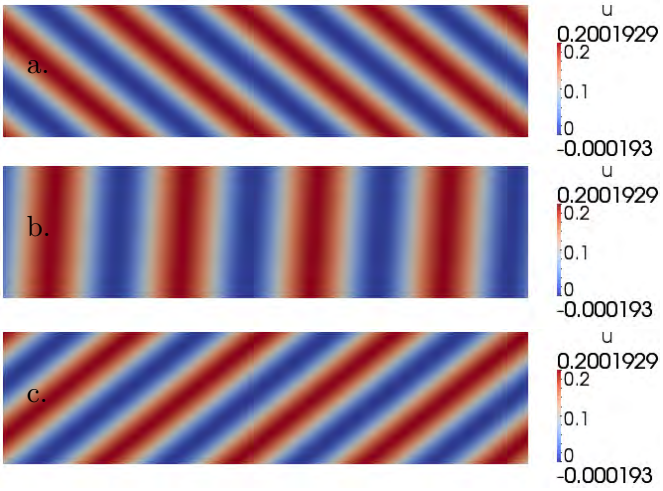

Figure 3: Evolution of a plane wave ($\alpha = 0$) with an initial wave-vector of $[\frac{4.0}{2\pi}, \frac{5.0}{2\pi}]$, after a total strain of (respectively) 0, 1.25, and 2.4375.

Typical sets of output data are given in figures 3 and 5. A comparison of the plane-wave amplitude at each point of total shear between our method and this analytical solution is given in figure 6; the evolution is qualitiatively similar, with a maximum of 5% error. However, our numerical solution is not symmetric, and reaches a maximum that is higher and sooner in strain than what is analytically predicted.

Our plane waves exhibit slight curving as the solution progresses; this is due mainly to the von Neumann condition used. That condition is not adequate because it artificially affects the shape of the waves in an unphysical manner.

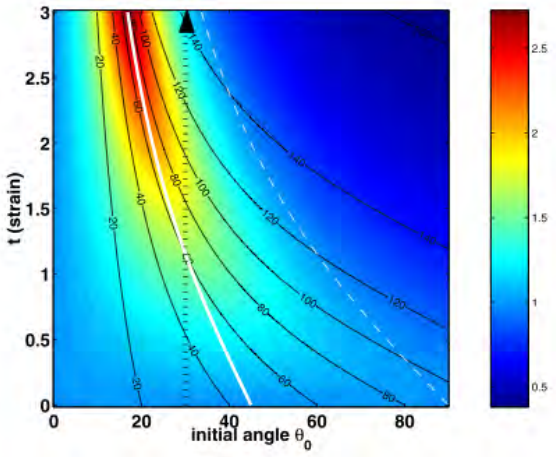

Figure 4: [*Spiegelman*, 2003] Plane wave amplitude $A(t, \phi_0)$ as a function of time (strain) and initial angle for $\alpha = -1$. Changing α only scales the magnitude of this image, not the angular dependence.

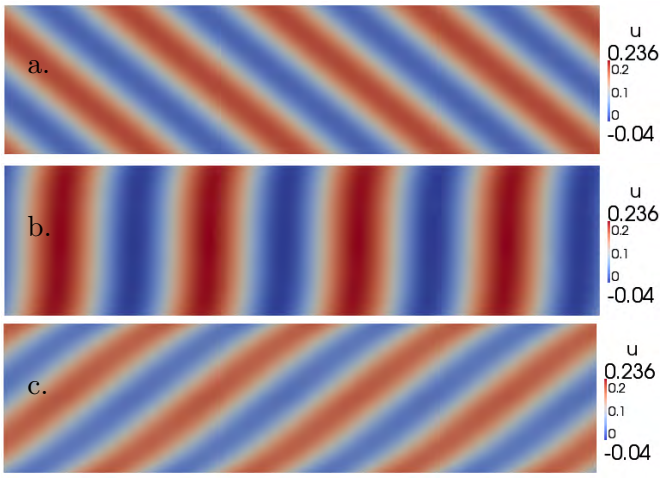

Figure 5: Evolution of a plane wave ($\alpha = -1$) with an initial wave-vector of $[\frac{4.0}{2\pi}, \frac{5.0}{2\pi}]$, after a total strain of (respectively) a. 0, b. 1.25, and c. 2.4375.

4 Linear Perturbation II: Random Initial Conditions

We also considered the behavior of the linearized equations when the initial condition was homogeneously random. The initial condition in this case was produced by arbitrarily picking a reference porosity, $\phi_0 = .25$, and adding uniform noise of amplitude $< 1\%$ of the reference porosity.

Allowing these equations to evolve did produce banding, as has been predicted, but the total porosity of the box grew exponentially over time (see figure 7). We expect that this effect is a result of the linearization, since it is not observed in similar calculations involving a fully nonlinear treatment (see figure 8). Moreover, the melt amplitude divergence calls into question the ability of this set of equations to accurately capture the dominant melt band angle; while it is possible in theory that the wave-vector of highest growth is different in the RIC case than the plane-wave initial case, the band created in this simulation did not evolve as has been proven that melt bands should (its wave-vector was stationary over time). It as such is probably some numerical instability instead of a natural consequence of the underlying physics.

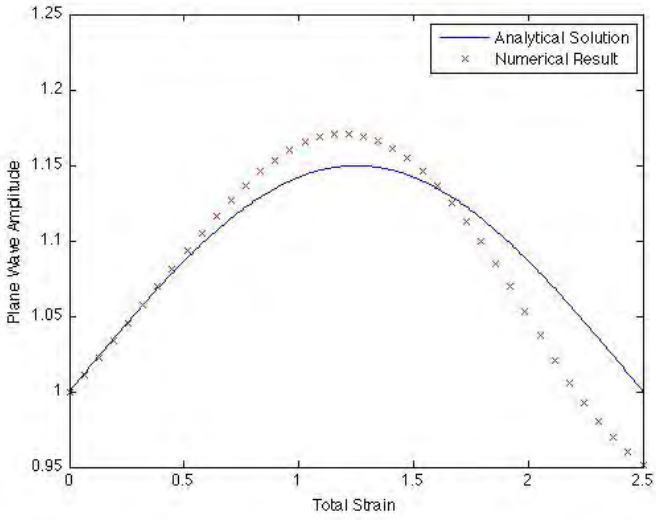

Figure 6: Comparison of numerical method to analytical solution of evolution of plane-wave amplitude for $\alpha = -1$.

5 Conclusion

We have evaluated the satisfactoriness of the linear form of the melt evolution equations for describing melt motion. They are lacking in key respects– notably, the evolution of the random initial condition is unphysical. This implies /that the behavior of rock rheology over time is influenced significantly by forces of order higher than the first, meaning that a full continuum model must include a nonlinear viscosity function for numerical stability and accuracy.

6 Further Study

In light of the apparent weakness of the linear approach, it has been shown that we must implement the nonlinear equations in order to faithfully sim-

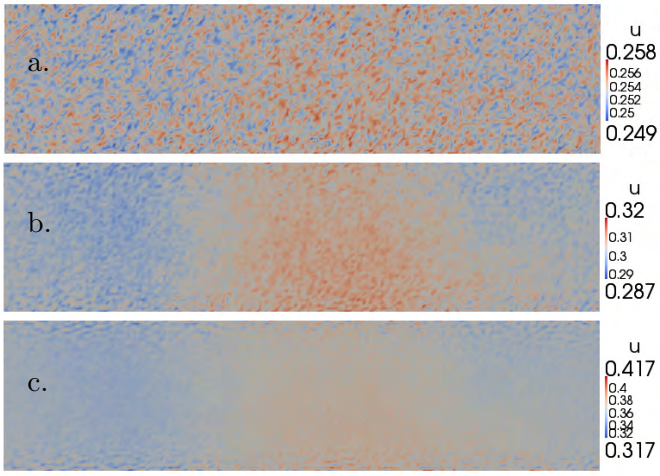

Figure 7: Evolution of random initial conditions ($\alpha = -1$) after a total strain of (respectively) a. .0625, b. .6875, and c. 1.3125.

ulate the equations for arbitrary initial conditions. This will allow us to handle the case of random initial conditions, and as such reliably quantify the extent of banding as a result of applied shear in nature.

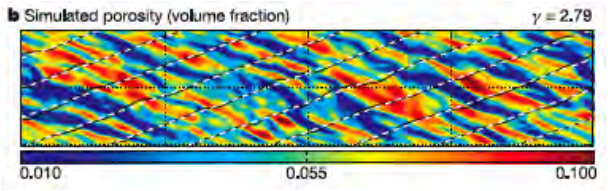

Figure 8: The porosity from a numerical simulation of the full nonlinear equations, using a power-law relationship for the aggregate viscosity to porosity. [*Katz et al.*, 2006]

More realistic numerical models will allow us to begin studying the way a representative volumetric element of crustal rock changes in viscosity as a result of applied shear. The theory of Backus averaging [*Backus*, 1962; *Gelinsky*, 1997] gives a theoretical basis for analyzing the rheological properties of a medium that has been well organized into layers of qualitatively different material: stress-strain relations are expressed as a full matrix, the components of which depend on a parameterization relying on layer porosity, permeability, and density, as well as fluid viscosity, density, and bulk modulus. Organization of a partially molten aggregate into bands is well characterized by a collection of layers that differ only (but markedly) in porosity, and therefore density. This approach is more satisfying in many respects than that which has already been used in this regard; Holtzmann's [*Holtzman et al.*, 2012] "segregation factor" formulation, for example, attempts to characterize segregation as one parameter S that varies between 0 and 1. Not only is S ill-defined as a function of the spatial variable ϕ–it relies instead on ϕ_b, the melt fraction in the bands, which one cannot determine satisfactorily solely from the porosity distribution–its effect on the rheology of the sample is not clear. As such, there is still a need in the literature for a precise elucidation of the segregation phenomenon's effect on the properties of the rock that exhibits it.

Once this has been accomplished, a full continuum model of the Earth that incorporates this viscosity effect may be built, and a theory of tectonics as driven by melt segregation may be thoroughly tested.

References

Backus, Long-wave elastic anisotropy produced by horizontal layering, *Journal of Geophysical Research*, *67*, 4427–4440, 1962.

Bercovici, Y. Ricard, and A. Richards Mark, The relation between mantle dynamics and plate tectonics: A primer, *The Hisroty and Dynamics of Global Plate Motions*, *121*, 5, 1969.

Gelinsky, S., Poroelastic backus averaging for anisotropic layered fluid- and gas-saturated sediments, *Geophysics*, *62*, 1867, 1997.

Holtzman, H. King Daniel S., and L. Kohlstedt David, Effects of stress-driven melt segregation on the viscosity of rocks, *Earth and Planetary Science Letters*, *359*, 184–193, 2012.

Katz, R. F., M. Spiegelman, and B. Holtzman, The dynamics of melt and shear localization in partially molten aggregates., *Nature*, *442*, 676–679, 2006.

Kohlstedt, and Holtzman, Shearing melt out of the earth: An experimentalist's perspective on the influence of deformation on melt extraction, *Annual Review of Earth and Planetary Sciences*, *37*, 561–593, 2009.

Spiegelman, M., Linear analysis of melt band formation by simple shear, *Geochemistry*, *4*, 8615, 2003.

Stevenson, Spontaneous small-scale melt segregation in partial melts undergoing deformation, *Geophysical Research Letters*, *16*, 1067–1070, 1989.

Tackley, Self-consistent generation of tectonic plates in three-dimensional mantle convection, *Earth and Planetary Science Letters*, *157*, 9, 1998.